

# Emulation of a Quantum Spin with a Superconducting Phase Qudit

Matthew Neeley, M. Ansmann, Radoslaw C. Bialczak, M. Hofheinz,  
Erik Lucero, A. D. O’Connell, D. Sank, H. Wang, J. Wenner,  
A. N. Cleland, Michael R. Geller, John M. Martinis\*

\*To whom correspondence should be addressed; E-mail: martinis@physics.ucsb.edu.

## Supporting Online Material

**Materials and Methods.** The phase qubit circuit used in this work has the following design circuit parameters: critical current  $I_0 \approx 2 \mu\text{A}$ , capacitance  $C \approx 1 \text{ pF}$ , and inductance  $L \approx 720 \text{ pH}$ . At the operating bias used in the experiment, the barrier height is  $\Delta U/\hbar\omega_p \approx 5.5$ . We use the lowest five states in the well for our qudit.

Microwave control signals are produced by a custom microwave arbitrary waveform generator (AWG), which modulates an input microwave source at frequency  $\omega_c$  using a two-quadrature (IQ) mixer. Quadrature voltage envelopes  $I(t)$  and  $Q(t)$  for the mixer are generated by a custom 1 ns resolution, 2-channel 14-bit digital-to-analog converter (DAC) card. The mixer takes the source signal  $\propto \cos(\omega_c t)$  and inputs  $I(t)$ ,  $Q(t)$  and produces an output signal  $\propto I(t) \cos(\omega_c t) + Q(t) \sin(\omega_c t)$ . Using envelopes  $I(t) + iQ(t) = A \exp(-i\delta\omega t)$ , the output signal is  $\propto A \cos((\omega_c + \delta\omega)t)$ , which is shifted from the original carrier frequency, a technique known as single-sideband mixing. By adding several such sideband-mixing envelopes, we obtain the desired multi-tone microwave control signal used to manipulate the qudit state from a single AWG. The DAC timing resolution and output filtering

determines the bandwidth accessible by sideband mixing, which in the current setup is  $\sim 600$  MHz, just enough to access all the relevant qudit transitions. Multiple AWG outputs with different carrier frequencies could be added to access a wider frequency range, if necessary.

For single-transition rotations, e.g.  $\pi$ - and  $\pi/2$ -pulses, the pulse envelope has length  $T = 16$ -ns and a shifted cosine shape  $A(t) = (A_{\max}/2)(1 - \cos(2\pi t/T))$  for  $0 \leq t \leq T$ . This gives the pulses a smooth turn-on and turn-off envelope and a full-width at half-max (FWHM) of 8 ns. While not as concentrated in frequency space as a gaussian, this shape has the advantage of going identically to zero at the endpoints, avoiding the need for truncation and allowing sequential pulses to be concatenated without additional delays. For spin-1 and spin-3/2 pulses, the emulated spin rotates more slowly than for single transitions, so an emulated spin  $\pi$ -rotation requires both qudit transitions to be driven through more than a  $\pi$ -rotation. This is done with a stretched pulse that consists of an 8 ns cosine turn on at the beginning, 8 ns cosine turn-off at the end, and constant amplitude  $A_{\max}$  drive in the middle, timed to achieve the desired total Rabi pulse area. This keeps the pulses shorter than increasing  $T$  alone, minimizing the effects of decoherence during the pulse; at the same time it keeps  $A_{\max}$  the same, avoiding unwanted AC Stark shifts at large drive amplitude and staying within the limited microwave dynamic range.

Qudit measurement requires that we choose appropriate measure-pulse amplitudes  $I_{\text{meas}}^{(n)}$  to maximize the discrimination between neighboring states (Fig. S1). This discrimination is characterized by the visibility, defined as the difference between tunneling probabilities of the upper and lower states. In this case, the  $|0\rangle$ - $|1\rangle$  visibility is 90%, while the  $|3\rangle$ - $|4\rangle$  visibility is just 66%. Note that these visibilities contain contributions from tunnelling as well as the imperfect state preparation due to  $T_1$  relaxation during the state preparation sequence.

To characterize the qudit, we measured the relaxation rates of the various states (Fig. S2). The measured rates are in fairly good agreement with the  $1/n$  scaling seen in a harmonic oscillator (S1). This is expected due to the relatively small anharmonicity of the potential at our operating point.

**Supplementary Text.** The Berry phase factor  $\exp(-im\Omega)$  acquired by a spin rotated about a closed bath was first predicted by Berry (S2) in the context of an adiabatically changing, non-degenerate Hamiltonian. Later treatments extended the theory to include degenerate Hamiltonians (S3). Here we show briefly that the adiabaticity requirement can also be dispensed with in the case of spin rotations, such as those emulated in the experiment.

In the derivation of Berry’s phase, one assumes a Hamiltonian  $\hat{H}(t)$  that varies cyclically in time. If the system starts in an eigenstate  $|m\rangle$  and stays in an eigenstate throughout the evolution, then at the end of one cycle, the system will again be in state  $|m\rangle$  but now multiplied by a phase factor

$$\exp(i\gamma_m) \exp\left\{-\frac{i}{\hbar} \int_0^T E_m dt\right\} \quad (\text{S1})$$

where the first term is the “geometric” phase (Berry phase) due to the changing Hamiltonian, and the second term is a “dynamical” phase due to the (time-dependent) energy of the eigenstate. For a spin, the Hamiltonian is simply  $\hat{H}(t) = \mathbf{B}(t) \cdot \hat{\mathbf{S}}$ , where  $\mathbf{B}(t)$  is a time-dependent magnetic field and  $\hat{\mathbf{S}}$  is the spin operator  $\hat{\mathbf{S}} = (\hat{S}_x, \hat{S}_y, \hat{S}_z)$ . As the state evolves, the quantization axis is chosen to be always along the instantaneous spin direction  $\langle \hat{\mathbf{S}} \rangle$ .

The requirement that a system starting in an eigenstate  $|m\rangle$  stay in an eigenstate as the Hamiltonian evolves is normally guaranteed by requiring the evolution to be adiabatic. For a spin, however, adiabaticity is not required. Suppose the system starts out in an

eigenstate of the spin operator, with the quantization along  $\langle \hat{\mathbf{S}} \rangle$  as mentioned above. This eigenvalue condition is

$$\langle \hat{\mathbf{S}} \rangle \cdot \hat{\mathbf{S}} |\psi\rangle = m |\psi\rangle. \quad (\text{S2})$$

Now, the spin is rotated by applying a magnetic field  $\mathbf{B}$ . The state evolution can be described in the Heisenberg picture where the spin operator evolves as

$$\frac{\partial \hat{\mathbf{S}}}{\partial t} = -i[\hat{\mathbf{S}}, \hat{H}] = \mathbf{B} \times \hat{\mathbf{S}}. \quad (\text{S3})$$

Differentiating the eigenvalue condition Eq. S2 and substituting in the time evolution Eq. S3 gives

$$\begin{aligned} \frac{\partial}{\partial t} (\langle \hat{\mathbf{S}} \rangle \cdot \hat{\mathbf{S}} |\psi\rangle) &= \frac{\partial \langle \hat{\mathbf{S}} \rangle}{\partial t} \cdot \hat{\mathbf{S}} |\psi\rangle + \langle \hat{\mathbf{S}} \rangle \cdot \frac{\partial \hat{\mathbf{S}}}{\partial t} |\psi\rangle \\ &= \langle \mathbf{B} \times \hat{\mathbf{S}} \rangle \cdot \hat{\mathbf{S}} |\psi\rangle + \langle \hat{\mathbf{S}} \rangle \cdot \mathbf{B} \times \hat{\mathbf{S}} |\psi\rangle \\ &= \mathbf{B} \times \langle \hat{\mathbf{S}} \rangle \cdot \hat{\mathbf{S}} |\psi\rangle - \mathbf{B} \times \langle \hat{\mathbf{S}} \rangle \cdot \hat{\mathbf{S}} |\psi\rangle \\ &= 0, \end{aligned}$$

where we have used vector triple product identities to cancel the terms. This means that the eigenvalue condition Eq. S2 will continue to hold even when the spin is rotated, regardless of adiabaticity. Hence the derivation of the geometric phase factor in Eq. S1 proceeds as in the adiabatic case, giving the familiar Berry phase  $\exp(i\gamma_m) = \exp(-im\Omega)$ .

To find the dynamic phase contribution to Eq. S1, recall that the qudit state is described in the rotating frame of moving eigenkets, as mentioned in the text. In this frame, all the spin states have zero energy, so that initially  $E_m = 0$ . At later times, the energy of a particular eigenstate is given by the projection of the magnetic field along the instantaneous spin axis which defines the quantization, that is

$$E_m \propto -m(\mathbf{B} \cdot \langle \hat{\mathbf{S}} \rangle). \quad (\text{S4})$$

Thus, if we require that the rotation axis, given by  $\mathbf{B}$ , is always perpendicular to the spin direction, that is  $\mathbf{B} \cdot \langle \hat{\mathbf{S}} \rangle = 0$ , then at all times  $E_m = 0$ , and the dynamical phase vanishes. This restricts the allowed spin rotations, as explained below, but simplifies the analysis since the phase accumulated during the rotation is entirely due to the geometric phase contribution.

As mentioned in the text, applied microwaves can rotate the emulated spin about any axis in the  $X$ - $Y$  plane, giving us control of  $B_x(t)$  and  $B_y(t)$ , with  $B_z(t) = 0$ . To avoid issues with dynamical phase, we also must satisfy the restriction just mentioned that the rotation axis be perpendicular to the spin direction. If the spin vector is on the  $Z$ -axis, either up or down, the rotation axis can be chosen as desired, since any vector in the  $X$ - $Y$  plane is perpendicular to  $Z$ ; however, if the spin state is not on the  $Z$ -axis, there is only one available perpendicular rotation axis in the  $X$ - $Y$  plane. Thus, once a rotation axis has been chosen and the spin has started to rotate away from the  $Z$ -axis, the rotation axis cannot be changed until the state again reaches the  $Z$ -axis in the opposite direction, corresponding to a rotation by angle  $\pi$ . This is the reason for applying successive  $\pi$ -pulses in the experiment. By changing the axis angle  $\Theta$  of the second  $\pi$ -rotation relative to the first, the spin can be made to trace out any desired solid angle, as demonstrated in the experiment.

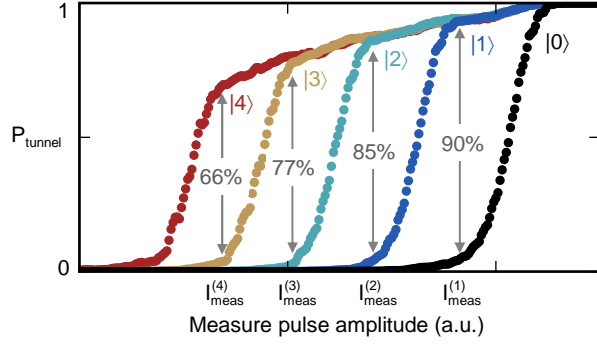


**Fig. S1.** Qudit measurement. Tunnelling probability is plotted versus measure-pulse amplitude after preparing the qudit in various states  $|n\rangle$  using successive  $\pi$ -pulses. Higher qudit states tunnel with weaker measure-pulses. The measure-pulse amplitudes  $I_{\text{meas}}^{(n)}$  are chosen to maximize the visibility, or difference in tunneling rates, between  $|n\rangle$  and  $|n - 1\rangle$ .

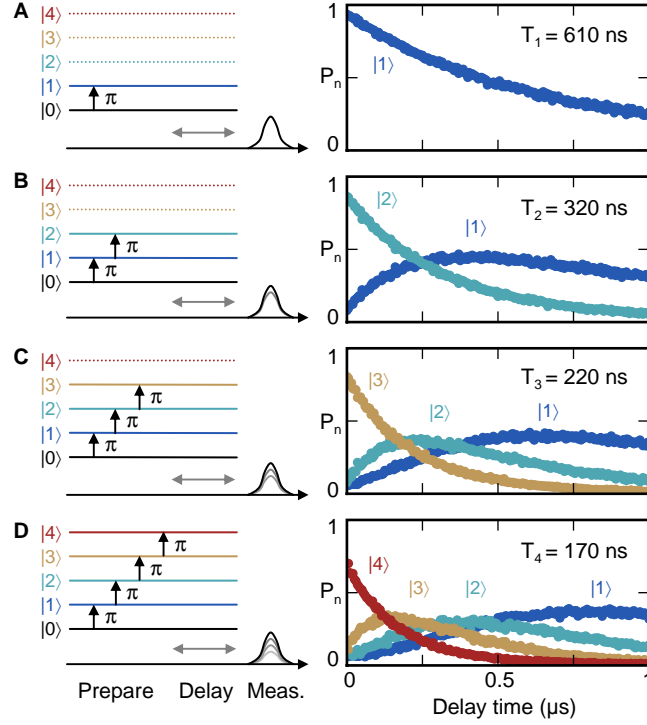


**Fig. S2.** Lifetime of qudit states. (A) Left, the microwave sequence used to measure the decay of  $|1\rangle$  is a single  $\pi$ -pulse, followed by a delay and finally measurement. Right, a plot of  $P_1$  versus time shows the decay of  $|1\rangle$  to the ground state, with a lifetime  $T_1 = 610$  ns. (B-D) Successive  $\pi$ -pulses are used to prepare  $|n\rangle$  and measure the decay rate  $T_n$ . The data on the left show  $P_n$  versus time. The higher states decay more quickly, in rough agreement with the harmonic oscillator prediction.

## References

- S1. H. Wang *et al.*, Phys. Rev. Lett. **101**, 240401 (2008).
- S2. M. V. Berry, Proc. R. Soc. Lond. A **392**, 45-57 (1984).
- S3. F. Wilczek and A. Zee, Phys. Rev. Lett. **52**, 2111-2114 (1984).